

# Compact dual-wavelength continuous-wave Er-doped fiber laser

SHI Jun-kai<sup>1</sup>, WANG Guo-ming<sup>1</sup>, JI Rong-yi<sup>1</sup>, ZHOU Wei-hu<sup>1,2\*</sup>

(1. *Laboratory of Laser Measurement Technology, Academy of Opto-Electronics, Chinese Academy of Sciences, Beijing 100094, China;*

2. *University of Chinese Academy of Sciences, Beijing 100049, China)*

\* *Corresponding author, E-mail:zhouweihu@aoe.ac.cn*

**Abstract:** Multiwavelength erbium-doped fiber lasers can be applied to many fields, such as wavelength division multiplexing optical communication and others attracting considerable attention. To meet the requirements of different applications, we propose a compact dual-wavelength continuous-wave erbium-doped fiber laser based on nonlinear amplifying loop mirror. An all-polarization-maintaining fiber cavity is adopted in which there are only three intracavity devices besides fiber itself: a wavelength division multiplexer, a  $2 \times 2$  fiber coupler and a fiber reflector. The intensity-dependent loss effect induced by the nonlinear amplifying loop mirror is used to equalize the intensity in the cavity. The input laser with higher power suffers a higher loss than the one with lower power. This feature can be used to suppress mode competition and achieve stable multiwavelength oscillation. With a pump power of 260 mW, dual-wavelength erbium-doped fiber laser can be achieved, with wavelengths of 1 560.5 nm and 1 563.2 nm, respectively. The side-mode suppression ratio is 46.8 dB. As pump power increases, the laser can operate in single-, dual- and triple-wavelength regions in proper order. As the multi-wavelength lasing oscillation is a balance between intensity-dependent loss and mode competition, the intensity change breaks the original balance state, resulting in the change in number and wavelength of lasing lines. This laser is simply structured and easy to operate. It can have applications in many fields.

**Key words:** fiber lasers; dual-wavelength operation; intensity-dependent loss; mode competition; nonlinear amplifying loop mirror

收稿日期:2018-09-21;修订日期:2018-11-16

基金项目:中国科学院国际合作局对外合作重点项目(No. 181811KYSB20160029);中国科学院前沿科学重点研究计划(No. QYZDY-SSW-JSC008)

Supported by the Key Project of Bureau of International Cooperation, Chinese Academy of Sciences (No. 181811KYSB20160029); the Key Research Project of Bureau of Frontier Sciences and Education, Chinese Academy of Sciences(No. QYZDY-SSW-JSC008)

# 结构紧凑的双波长连续波掺铒光纤激光器

石俊凯<sup>1</sup>, 王国名<sup>1</sup>, 纪荣祎<sup>1</sup>, 周维虎<sup>1,2\*</sup>

(1. 中国科学院光电研究院 激光测量技术研究室, 北京 100094;

2. 中国科学院大学, 北京 100049)

**摘要:**多波长掺铒光纤激光器在波分复用光学通信等领域具有广阔的应用前景, 引起了大量关注。为了满足不同场合的应用需求, 本文报道了一种结构紧凑、基于非线性放大光纤环境的双波长连续运转掺铒光纤激光器。该激光器采用全保偏光纤结构。除了光纤外, 激光腔内只含有波分复用器、 $2 \times 2$  光纤耦合器和光纤反射镜 3 个器件。非线性放大光纤环境在腔内引入强度相关损耗, 当腔内损耗随着入射光强增加而增加时, 可以有效抑制腔内激光模式竞争。当强度相关损耗的抑制作用和激光模式竞争达到平衡时, 激光器即可实现稳定的多波长输出。在 260 mW 泵浦功率下, 激光器运转在双波长振荡状态, 输出波长分别为 1 560.5 nm 和 1 563.2 nm, 边模抑制比达到 46.8 dB。随着泵浦功率的提高, 激光器依次工作在单波长、双波长和三波长运转状态。该激光器结构简单, 操作方便, 具有很好的应用前景。

**关键词:** 光纤激光器; 双波长运转; 强度相关损耗; 模式竞争; 非线性放大光纤环境

**中图分类号:** TN242 **文献标识码:** A **doi:** 10.3788/CO.20191204.0810

## 1 Introduction

In recent years, multi-wavelength Erbium-Doped Fiber (EDF) lasers have attracted a large amount of attentions<sup>[1-5]</sup>. Compared with methods using a large number of single-wavelength lasers, multi-wavelength lasers can reduce the complexity, development and maintenance cost of lasers. They also have broad application prospects in wavelength-division multiplexing free-space optical communication and optical fiber communication systems. Multi-wavelength EDF lasers are also useful in fiber optic sensing, fiber device inspection, optical signal processing and microwave signal generation.

Since the uniform broadening effect of an EDF causes mode competition, EDF lasers generally cannot achieve stable multi-wavelength operation at room temperature. In order to achieve multi-wavelength operation, S. Yamashita *et al.* used liquid nitrogen to cool an EDF to 77 K and the gain spectrum width of the EDF reduced to about 1 nm, ultimately achieving stable multi-wavelength output<sup>[6]</sup>. However, this cryogenic cooling method requires strict ex-

perimental conditions, which is not conducive to practical applications. In order to achieve stable multi-wavelength output at room temperature, various methods have been proposed to suppress mode competition in EDF lasers in addition to using a dual-core EDF with a non-uniform broadening effect<sup>[7]</sup>. The most common method is introducing comb spectral filter in the laser cavity, such as Fabry Perot etalon<sup>[8-10]</sup>, Mach Zehnder interferometer<sup>[11-13]</sup>, specially designed fiber Bragg grating<sup>[14-15]</sup>, among others. Using comb filter can overcome the uniform broadening effect of an EDF and achieve stable multi-wavelength operation. In addition to comb filters, people have used nonlinear fiber effects<sup>[16-19]</sup>, cascaded or arrayed fiber Bragg gratings<sup>[20-22]</sup>, polarization hole burning effects<sup>[23-24]</sup> and spatial mode beat frequency effects<sup>[25-27]</sup> to successively achieve a multi-wavelength EDF laser. In recent years, the intensity-dependent loss mechanisms have been introduced into EDF lasers, such as nonlinear polarization rotation effect<sup>[28-30]</sup>, Nonlinear Optical Loop Mirror (NOLM)<sup>[31-33]</sup>. The intensity-dependent loss is used to suppress mode competition and achieve multi-wavelength simultaneous oscillation. However,

most of these intensity-dependent loss mechanisms combining with other mechanisms or manual adjustment devices are needed to achieve stable multi-wavelength operation. This makes the structure of the light source more complicated and inconvenient to use.

In this paper, a dual-wavelength continuous-wave EDF laser using a Nonlinear Amplifying Loop Mirror (NALM) is constructed. The laser adopts an all Polarization-Maintaining (PM) fiber structure and has high environmental stability. In addition to the optical fiber, there are only three devices in the cavity: Wavelength Division Multiplexer (WDM),  $2 \times 2$  fiber coupler, and fiber reflector. The structure is simple. With the pump power of 260 mW, the laser operates in dual-wavelength region with output wavelengths of 1 560.5 nm and 1 563.2 nm, respectively, and the side mode suppression ratio is 46.8 dB. It has also been observed in the experiment that the laser can operate in single-, dual- and triple-wavelength states as the pump power increases.

## 2 Experimental Setup and Working Principle

The experimental setup of the dual-wavelength EDF laser is shown in Fig. 1. A  $2 \times 2$  PM fiber Optical Coupler (OC) was used as the junction of the laser and the splitter ratio of OC was 40 : 60. The NALM is formed with a piece of PM EDF (PM-ESF-7/125). A 976 nm Laser Diode (LD) delivering a maximum output power of 800 mW is used as a pump source. The pump laser is coupled into the cavity through a standard PM 976/1 550 nm WDM. The linear arm of the cavity consists of a PM fiber. High Reflector (HR). The laser beam transmitting through the NALM is utilized as Output (OP). Since the uniform broadening effect of the EDF causes mode competition, the EDF laser generally cannot achieve stable multi-wavelength continuous-wave operation at room temperature. The NALM in this

scheme can suppress the mode competition.

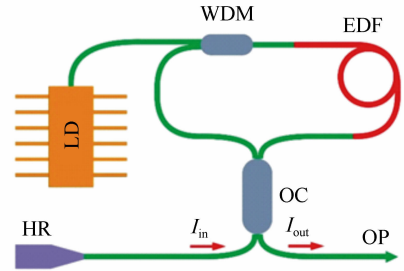


Fig. 1 Experimental setup of dual wavelength EDF laser: LD, laser diode; WDM, wavelength division multiplexer; EDF, Er-doped fiber; OC, optical coupler; HR, high reflector; OP, output  
图 1 双波长掺铒光纤激光器实验装置图: LD, 激光二极管; WDM, 波分复用器; EDF, 掺铒光纤; OC, 光学耦合器; HR, 高反射器; OP, 输出

Fig. 2 is a schematic diagram of the NOLM. The incident laser beam light passes through the OC and is split into two beams, transmitting in opposite directions. The splitting ratio of the coupler is  $\alpha$ ;  $(1 - \alpha)$ , where  $0 < \alpha \leq 0.5$ .

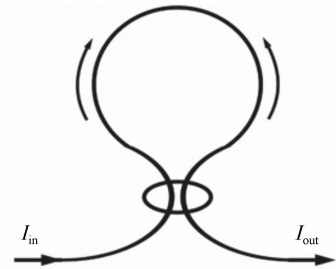


Fig. 2 Schematic diagram of a nonlinear optical loop mirror

图 2 非线性光纤环镜原理示意图

The two beams pass through the fiber loop in clockwise and counterclockwise directions, then each of them is divided into two beams by the coupler, interference occurs at the input and output ports of the NOLM to form the reflected laser and transmitted laser. Transmittance of NOLM is defined as the ratio of the output laser intensity  $I_{out}$  to the input laser intensity  $I_{in}$ , which is expressed as<sup>[34]</sup>

$$T = I_{out}/I_{in} = 1 - 2\alpha(1 - \alpha)(1 + \cos\Delta\psi), \quad (1)$$

where  $\Delta\psi$  is the phase difference accumulated when the two beams transmitted in the opposite direction of the fiber loop, and can be expressed as  $\Delta\psi = (\Delta I \times 2\pi n_2 L) / \lambda = ((1 - 2\alpha) I_{in} \times 2\pi n_2 L) / \lambda$ ;  $\Delta I$  is the intensity difference of the two beams,  $L$  is the length of the fiber loop,  $n_2$  is the nonlinear coefficient of the fiber, and  $\lambda$  is the laser wavelength. Assuming  $\alpha = 0.4$ , the transmittance as a function of the phase difference  $\Delta\psi$  is shown in Fig. 3. It can be seen that the transmittance of the NOLM exhibits a periodic change as the phase difference increases. When  $\alpha < 0.5$ , the phase difference  $\Delta\psi$  is proportional to the input laser intensity  $I_{in}$ . That is, the transmittance changes periodically as the input laser intensity  $I_{in}$  increases. The NOLM is used as the end mirror to form the resonant cavity, and the intensity-dependent loss can then be introduced. When the phase difference  $\Delta\psi$  satisfies  $2n\pi \leq \Delta\psi < (2n + 1)\pi$  ( $n = 0, 1, 2, \dots$ ), the intracavity loss increases as the incident light intensity increases. This effect can suppress laser mode competition in the cavity<sup>[34]</sup>. When the suppression and laser mode competition are balanced, the laser can achieve multi-wavelength oscillation. The NALM can play the same role as NOLM.

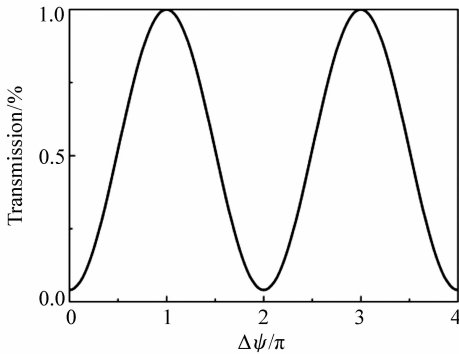


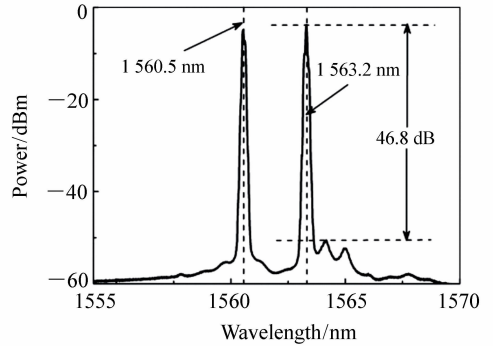
Fig. 3 Transmission as a function of the phase difference  
图3 透射率与相位差的关系曲线

In addition, the gain-imbalance in the fiber loop can increase the light intensity difference between the two beams transmitted in the opposite direction, and accelerate the accumulation of the

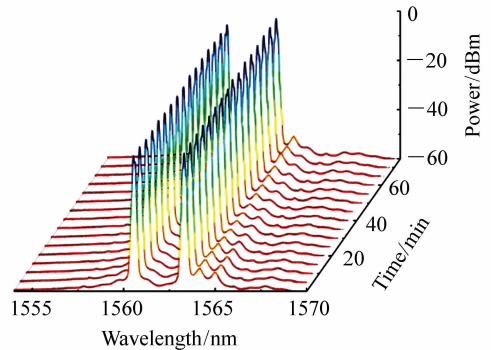
phase difference. Since the laser operates in the continuous-wave output state, the laser power density in the cavity is low. The phase difference  $\Delta\psi$  is between 0 and  $\pi$ .

### 3 Experimental Results

The laser was constructed using the scheme in Fig. 1. The laser output spectrum was measured using a spectrum analyzer (YOKOGAWA AQ6370D) with a spectral resolution of 0.02 nm. When the pump power was 260 mW, the laser output power was 13.2 mW. The output spectrum is shown in Fig. 4(a). The two wavelengths of 1560.5 nm and 1563.2 nm are simultaneously oscillated in the la-



(a) 双波长输出光谱  
(a) Dual-wavelength output spectrum



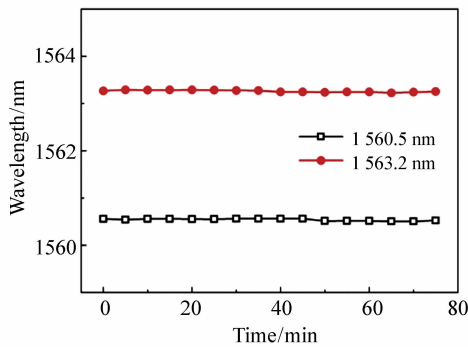
(b) 75 min 内重复扫描的光谱 (扫描间隔为 5 min)  
(b) Repeatedly scanned output spectra with 5 min interval in 75 minutes

Fig. 4 Characteristics of output spectra  
图4 激光器输出光谱特性

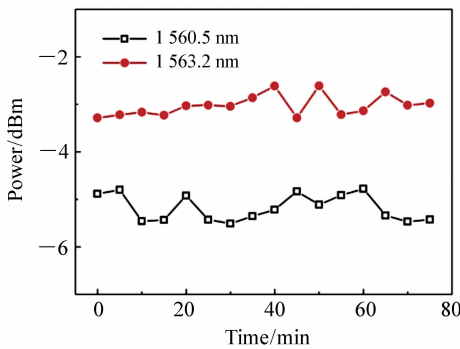
ser, and the power difference is about 1.6 dB. The two wavelengths were spaced 2.7 nm apart and the

side mode suppression ratio was greater than 45 dB. The output spectrum was scanned 16 times in succession with a scanning interval of 5 minutes. Fig. 4 (b) is the laser output spectra at different times. The results show that there is no significant change in the center wavelength and power within a period of 75 minutes.

In order to further reveal the stability of the dual-wavelength output of the laser at room temperature, the central wavelengths and powers of the two wavelengths of the laser output are recorded within 75 minutes, as shown in Fig. 5. It can be seen that, the fluctuations of the two center wavelengths at 1 560.5 nm and 1 563.2 nm are essentially the same at 0.06 nm and the power fluctuation range is less than 0.8 dB and 0.7 dB. This slight power



(a) 波长偏移  
(a) Wavelength drift



(b) 功率波动  
(b) Power fluctuation

Fig. 5 Laser output stability

图 5 激光器输出稳定性

fluctuation is mainly caused by the intensity noise of the pump laser and the temperature-sensitive cavity

loss. The laser shows good stability.

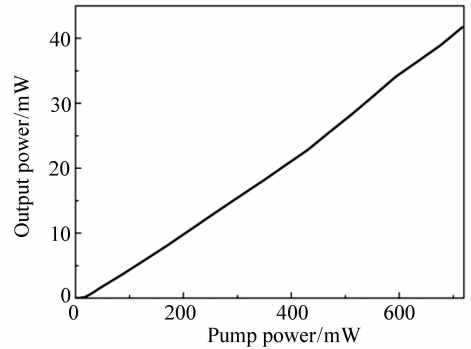


Fig. 6 Output power as a function of pump power

图 6 激光器斜效率曲线

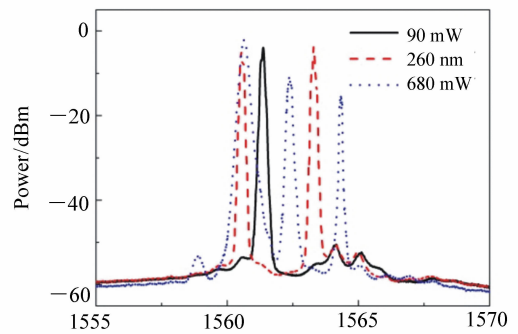


Fig. 7 Output spectra versus different pump powers

图 7 不同泵浦功率下的输出光谱

In the experiment, it was also discovered that as the pump power increased, the number of wavelength oscillating simultaneously in the cavity also increased. Fig. 6 shows the output power as a function of pump power. The laser power was measured by the power meter (Thorlabs, PM100D). As shown, the pump threshold was approximately 20 mW and the output power increased linearly with pump power increased. The conversion efficiency was approximately 6.1%. Fig. 7 shows the output spectra with pump powers of 90 mW, 260 mW and 680 mW. When the pump power is low, the laser power density in the cavity is weak and the intensity-related loss is insufficient to suppress the mode competition in the cavity. Therefore, the laser operates in a single wavelength state, as shown by the solid line in Fig. 7. As the pump power increases, the laser pow-

er density in the cavity increases gradually and the intensity-dependent loss effect becomes able to suppress the competition between more modes. The laser can then operate in a dual-wavelength or a triple-wavelength state, as shown in dashed line and dotted line in Fig. 7. In a previous report, the intracavity operating wavelength number can be adjusted by changing the intracavity polarization controller state<sup>[30]</sup> or the fiber loop radius<sup>[10]</sup>.

## 4 Conclusion

In this paper, a compact dual-wavelength continuous-wave EDF laser was constructed. The laser utilizes an all-PM fiber structure wherein there are

——中文对照版——

## 1 引言

近年来,多波长掺铒光纤激光器引起了大量关注<sup>[1-5]</sup>。相比于采用大量单波长激光器的方法,多波长激光器可以降低激光器的复杂度、系统成本和维护成本,在波分复用自由空间光学通信和光学光纤通信系统中具有广阔的应用前景。多波长掺铒光纤激光器还被应用于光纤光学传感、光纤器件检测、光学信号处理和微波信号产生等领域。

由于掺铒光纤的均匀展宽效应会引起模式竞争,所以通常掺铒光纤激光器在室温下不能实现稳定的多波长运转。为了实现多波长运转,S. Yamashita 等人采用液氮将掺铒光纤冷却到 77 K,掺铒光纤的增益谱宽随之降低到约 1 nm,最终实现了稳定的多波长输出<sup>[6]</sup>。但是低温冷却方法对实验条件要求较高,不利于实际应用。为了实现室温下稳定的多波长输出,人们除了采用具有非均匀展宽效应的双芯掺铒光纤构建激光器<sup>[7]</sup>外,还提出了各种各样的方法来抑制掺铒光纤激光器中的模式竞争。其中最常用的方法是在激光腔内引入梳状光谱滤波器,如法布里珀罗标准具<sup>[8-10]</sup>、

only three devices in the cavity in addition to the fiber itself: WDM, 2 × 2 OC and HR. The intensity-dependent loss introduced by the NALM is utilized to suppress the mode competition. When the pump power is 260 mW, the laser operates in a dual-wavelength oscillation state with output wavelengths of 1 560.5 nm and 1 563.2 nm and has a side mode suppression ratio greater than 45 dB. Within 75 minutes, both wavelengths ranged in 0.06 nm with power fluctuations less than 0.8 dB and 0.7 dB. As the pump power increases, the laser operates in single-, dual-, and triple-wavelength modes. The laser is compact and easy to operate, so it has many applications.

马赫泽德干涉仪<sup>[11-13]</sup>、特殊设计的光纤布拉格光栅<sup>[14-15]</sup>等。梳状滤波器可以克服掺铒光纤的均匀展宽效应,实现稳定的多波长运转。除了梳状滤波器以外,人们利用光纤非线性效应<sup>[16-19]</sup>、级联或阵列式光纤布拉格光栅<sup>[20-22]</sup>、偏振烧孔效应<sup>[23-24]</sup>、空间模式拍频效应<sup>[25-27]</sup>等方法相继实现了多波长运转的掺铒光纤激光器。近年来,人们将强度相关损耗机制引入掺铒光纤激光器,如非线性偏振旋转效应<sup>[28-30]</sup>和非线性光纤环镜<sup>[31-33]</sup>,利用强度相关损耗抑制模式竞争,实现了多波长同时振荡。但是强度相关损耗机制大多需要结合其他机制,或引入手动调节器件才能实现稳定的多波长运转。这就使得光源结构更为复杂,不便于使用。

本文构建了一种基于非线性放大光纤环境的双波长连续运转掺铒光纤激光器。该激光器采用全保偏光纤结构,环境稳定性高。除光纤外,腔内只有波分复用器(WDM)、耦合器、光纤反射镜 3 个器件,结构简单。当泵浦功率为 260 mW 时,激光器运转在双波长振荡状态,输出波长分别为 1 560.5 nm 和 1 563.2 nm,边模抑制比为 46.8 dB。实验中还观察到,随着泵浦功率的增加,激光器可以工作在单波长、双波长和三波长运转状态。

## 2 实验装置与工作原理

双波长掺铒光纤激光器实验装置如图 1 所示。采用  $2 \times 2$  保偏光纤光学耦合器(OC)作为激光器的枢纽,耦合器的分束比为 40:60。将耦合器一端的两根尾纤连接,形成光纤环路。对于耦合器的另一端,其中一根尾纤连接保偏光纤反射器(HR),与光纤环境构成谐振腔;另一根尾纤悬空,作为激光器的耦合输出(OP)。增益光纤采用 Nufern 公司生产的 PM-ESF-7/125 型保偏掺铒光纤(EDF),并置于光纤环路内,构成非线性放大光纤环境。泵浦源采用尾纤耦合输出的单模激光二极管(LD),最大输出功率为 800 mW,中心波长为 976 nm。泵浦光通过保偏尾纤 WDM 耦合进增益光纤,实现激光增益。由于掺铒光纤的均匀展宽效应会引起腔内激光模式竞争,通常掺铒光纤激光器在室温下不能实现稳定的多波长连续波运转。而本方案中的非线性放大光纤环境可以起到抑制模式竞争的作用。

图 2 为非线性放大光纤环境原理示意图。入射光经过耦合器后分为沿相反方向传输的两束光,耦合器的分束比为  $\alpha:(1-\alpha)$ ,其中  $0 < \alpha \leq 0.5$ 。两束光分别沿着顺时针和逆时针方向通过光纤环路后,各自经过耦合器分为两束,分别在光纤环境输入端和输出端发生干涉,形成环境的反射光和透射光。这里只讨论非线性光纤环境的透射率。透射率的定义为输出光强  $I_{\text{out}}$  与输入光强  $I_{\text{in}}$  的比值,其表达式为<sup>[34]</sup>:

$$T = I_{\text{out}}/I_{\text{in}} = 1 - 2\alpha(1-\alpha)(1 + \cos\Delta\psi), \quad (1)$$

其中,  $\Delta\psi$  为沿相反方向传输的两束光经过光纤环路后积累的相位差,可表达为  $\Delta\psi = (\Delta I * 2\pi n_2 L)/\lambda = ((1-2\alpha)I_{\text{in}} * 2\pi n_2 L)/\lambda$ ,  $\Delta I$  为两束光的光强差,  $L$  为光纤环路长度,  $n_2$  为光纤非线性系数,  $\lambda$  为激光波长。取  $\alpha = 0.4$ , 透射率随相位差  $\Delta\psi$  的变化曲线如图 3 所示。可以看到,非线性光纤环境的透射率随着相位差的增加呈现出周期性的变化。当  $\alpha < 0.5$  时,相位差  $\Delta\psi$  正比于输入光强  $I_{\text{in}}$ , 即透射率随输入光强  $I_{\text{in}}$  的增加呈周期

性变化。以非线性光纤环境作为端镜构成谐振腔,即可引入强度相关损耗。相位差  $\Delta\psi$  满足  $2n\pi \leq \Delta\psi < (2n+1)\pi$  ( $n=0,1,2,\dots$ ) 时,腔内损耗随着入射光强的增加而增加。对于强度较大的输入光,激光腔的损耗较大;而对于强度较小的输入光,激光腔的损耗也较小。这一作用可以有效地抑制腔内激光模式竞争<sup>[34]</sup>。当这种抑制作用和激光模式竞争达到平衡时,激光器即可以实现多个波长同时振荡。非线性放大光纤环境可以起到与非线性光纤环境相同的作用。此外光纤环路中的增益可以提高沿相反方向传输的两束光的光强差,加快相位差的积累。由于激光器工作在连续波输出状态,腔内激光功率密度较低,因此产生的相位差  $\Delta\psi$  处于 0 与  $\pi$  之间。

## 3 实验结果

采用图 1 中的方案构建激光器,实验中使用 YOKOGAWA 公司的光谱分析仪 AQ6370D 测量激光器输出光谱,光谱分辨率为 0.02 nm。当泵浦功率为 260 mW 时,激光器输出功率为 13.2 mW,输出光谱如图 4(a)所示。可以看到,激光器内 1 560.5 nm 和 1 563.2 nm 两个波长同时振荡,功率相差约为 1.6 dB,两个波长输出功率均衡。两个波长的间隔为 2.7 nm,边模抑制比均大于 45 dB。对输出光谱连续扫描了 16 次,扫描间隔为 5 min。图 4(b)为不同时间激光器输出的光谱图。测量结果显示,在 75 min 内激光器输出的两个波长的中心波长和功率并未出现明显的变化。

为了进一步揭示室温下激光器双波长输出的稳定性,记录了激光器两个输出波长的中心波长和功率随时间的变化情况,如图 5 所示。可以看到,在 75 min 内,1 560.5 nm 和 1 563.2 nm 处两个中心波长的波动范围基本一致,为 0.06 nm,功率波动范围分别小于 0.8 dB 和 0.7 dB。轻微的功率变化主要是由泵浦光的强度噪声和温度扰动引起的腔内损耗变化共同造成的。实验结果显示,激光器具有良好的稳定性。

实验中还发现,随着泵浦功率的增加,激光腔内同时振荡的波长数也随之增加。图 6 为激光器

斜效率曲线。激光功率由功率计(Thorlabs, PM100D)测量。如图6所示,激光器的工作阈值约为20 mW,输出功率随泵浦功率的增加呈线性增加,激光器斜率效率约为6.1%。图7为泵浦功率分别为90、260和680 mW条件下的输出光谱。当泵浦功率较低时,腔内运转的激光功率密度较弱,产生的强度相关损耗作用不足以抑制腔内的模式竞争,因此激光器运转在单波长状态,如图7中黑色实线所示。随着泵浦功率的提高,腔内运转的激光功率密度逐渐增强,产生的强度相关损耗作用可以抑制更多模式之间的竞争,激光器可以运转在双波长和三波长状态,如图7中虚线和点线所示。在之前的报道中,有人提出通过改变腔内偏振控制器状态<sup>[30]</sup>或光纤弯曲半径<sup>[10]</sup>调节腔内损耗,同样可以实现腔内运转波长数量的调节。

## 4 结 论

本文构建了一种结构紧凑的双波长连续运转掺铒光纤激光器。该激光器采用全保偏光纤结构,除了光纤外,腔内只有WDM、2×2光纤耦合器和光纤反射器3个器件。利用非线性放大光纤环境引入的强度相关损耗抑制模式竞争,实现双波长运转。当泵浦功率为260 mW时,激光器运转在双波长振荡状态,输出波长分别为1560.5 nm和1563.2 nm,边模抑制比大于45 dB。在75 min内,两个波长的波动范围均为0.06 nm,功率波动范围分别小于0.8 dB和0.7 dB。随着泵浦功率的增加,激光器分别工作在单波长、双波长和三波长运转状态。该激光器结构紧凑,操作方便,可应用于不同的工作场合。

## 参考文献:

- [1] 姜明顺,冯德军,隋青美. 机械感生长周期光纤光栅的可调谐环形光纤激光器[J]. 光学精密工程,2010,18(2):311-316.  
JIANG M SH, FENG D J, SUI Q M. Tunable ring fiber laser using mechanical-induced long-period fiber grating[J]. *Opt. Precision Eng.*, 2010, 18(2): 311-316. (in Chinese)
- [2] 董繁龙,赵方舟,葛廷武,等. 全光纤激光器光束质量的优化[J]. 光学精密工程,2014,22(4):844-849.  
DONG F L, ZHAO F ZH, GE T W, et al.. Optimization of beam quality for all-fiber lasers[J]. *Opt. Precision Eng.*, 2014, 22(4): 844-849. (in Chinese)
- [3] 许阳,康喆,贾志旭,等. 基于金纳米棒可饱和吸收体的被动调Q掺铒光纤激光器[J]. 发光学报,2013,34(12):1631-1635.  
XU Y, KANG ZH, JIA ZH X, et al.. Passively Q-switched Er-doped fiber lasers by using gold nanorods as saturable absorbers[J]. *Chinese Journal of Luminescence*, 2013, 34(12): 1631-1635. (in Chinese)
- [4] 孟祥伟,姚传飞,王善德,等.  $Tm^{3+}/Ho^{3+}$ 共掺碲酸盐微结构光纤激光器[J]. 发光学报,2015,36(1):94-98.  
MENG X W, YAO CH F, WANG SH D, et al..  $Tm^{3+}/Ho^{3+}$  co-doped tellurite microstructure fiber lasers[J]. *Chinese Journal of Luminescence*, 2015, 36(1): 94-98. (in Chinese)
- [5] 康喆,刘明奕,刘承志,等. 基于微纳光纤-单壁碳纳米管可饱和吸收体的被动调Q掺铒光纤激光器[J]. 发光学报,2017,38(5):630-635.  
KANG ZH, LIU M Y, LIU CH ZH, et al.. Passively Q-switched  $Yb^{3+}$ -doped fiber laser based on microfiber-single wall carbon nanotube saturable absorber[J]. *Chinese Journal of Luminescence*, 2017, 38(5): 630-635. (in Chinese)
- [6] YAMASHITA S, HOTATE K. Multiwavelength erbium-doped fiber laser using intracavity etalon and cooled by liquid nitrogen[J]. *Electronics Letters*, 1996, 32(14): 1298-1299.
- [7] GRAYDON O, LOH W H, LAMING R I, et al.. Triple-frequency operation of an Er-doped twincore fiber loop laser[J]. *IEEE Photonics Technology Letters*, 1996, 8(1): 63-65.
- [8] PAN SH L, LOU C Y, GAO Y Z. Multiwavelength erbium-doped fiber laser based on inhomogeneous loss mechanism by use of a highly nonlinear fiber and a Fabry-Perot filter[J]. *Optics Express*, 2006, 14(3): 1113-1118.



- [9] HE X Y, FANG X, LIAO CH R, *et al.*. A tunable and switchable single-longitudinal-mode dual-wavelength fiber laser with a simple linear cavity[J]. *Optics Express*, 2009, 17(24):21773-21781.
- [10] ESTUDILLO-AYALA J M, JAUREGUI-VAZQUEZ D, HAUS J W, *et al.*. Multi-wavelength fiber laser based on a fiber Fabry-Perot interferometer[J]. *Applied Physics B*, 2015, 121(4):407-412.
- [11] QURESHI K K. Switchable dual-wavelength fiber ring laser featuring twin-core photonic crystal fiber-based filter[J]. *Chinese Optics Letters*, 2014, 12(2):020605.
- [12] MA W ZH, WANG T SH, ZHANG P, *et al.*. Widely tunable multiwavelength thulium-doped fiber laser using a fiber interferometer and a tunable spatial mode-beating filter[J]. *Applied Optics*, 2015, 54(12):3786-3791.
- [13] GUTIERREZ-GUTIERREZ J, ROJAS-LAGUNA R, ESTUDILLO-AYALA J M, *et al.*. Switchable and multi-wavelength linear fiber laser based on Fabry-Perot and Mach-Zehnder interferometers[J]. *Optics Communications*, 2016, 374:39-44.
- [14] DONG X Y, SHUM P, NGO N Q, *et al.*. Multiwavelength Raman fiber laser with a continuously-tunable spacing[J]. *Optics Express*, 2006, 14(8):3288-3293.
- [15] 杨秀峰, 方秀丽, 童峥嵘, 等. 基于相移光栅的多波长掺铒光纤激光器的实验研究[J]. *中国激光*, 2012, 39(6):0602012.  
YANG X F, FANG X L, TONG ZH R, *et al.*. Experimental study of multi-wavelength fiber laser based on phase-shifted fiber grating[J]. *Chinese Journal of Lasers*, 2012, 39(6):0602012. (in Chinese)
- [16] WANG P H, WENG D M, LI K, *et al.*. Multi-wavelength erbium-doped fiber laser based on four-wave-mixing effect in single mode fiber and high nonlinear fiber[J]. *Optics Express*, 2013, 21(10):12570-12578.
- [17] AL-ALIMI A W, YAACOB M H, ABAS A F, *et al.*. 150-channel four wave mixing based multiwavelength Brillouin-erbium doped fiber laser[J]. *IEEE Photonics Journal*, 2013, 5(4):1501010.
- [18] WANG X R, YANG Y F, LIU M, *et al.*. Frequency spacing switchable multiwavelength Brillouin erbium fiber laser utilizing cascaded Brillouin gain fibers[J]. *Applied Optics*, 2016, 55(23):6475-6479.
- [19] WEI Y ZH, YANG X, MAO B M, *et al.*. Channel-spacing tunable multiwavelength thulium-doped fiber laser based on four-wave mixing effect in a high nonlinear fiber[J]. *Microwave and Optical Technology Letters*, 2016, 58(2):337-339.
- [20] ÁLVAREZ-TAMAYO R I, DURÁN-SÁNCHEZ M, POTTIEZ O, *et al.*. A dual-wavelength tunable laser with superimposed fiber Bragg gratings[J]. *Laser Physics*, 2013, 23(5):055104.
- [21] ROTA-RODRIGO S, RODRÍGUEZ-COBO L, QUINTELA M Á, *et al.*. Dual-wavelength single-longitudinal mode fiber laser using phase-shift Bragg gratings[J]. *IEEE Journal of Selected Topics in Quantum Electronics*, 2014, 20(5):0900305.
- [22] YANG W, LU P, WANG SH, *et al.*. A novel switchable and tunable dual-wavelength single-longitudinal-mode fiber laser at 2  $\mu\text{m}$ [J]. *IEEE Photonics Technology Letters*, 2016, 28(11):1161-1164.
- [23] FENG S CH, XU O, LU SH H, *et al.*. Switchable single-longitudinal-mode dual-wavelength erbium-doped fiber ring laser based on one polarization-maintaining fiber Bragg grating incorporating saturable absorber and feedback fiber loop[J]. *Optics Communications*, 2009, 282(11):2165-2168.
- [24] ZHANG CH F, SUN J, JIAN SH SH, *et al.*. A new mechanism to suppress the homogeneous gain broadening for stable multi-wavelength erbium-doped fiber laser[J]. *Optics Communications*, 2013, 288:97-100.
- [25] 郝艳萍, 张书敏, 王新占, 等. 基于多模光纤滤波器的可调谐掺铒光纤激光器[J]. *光学学报*, 2011, 31(8):0814006.  
HAO Y P, ZHANG SH M, WANG X ZH, *et al.*. Tunable Erbium-doped fiber laser based on multi-mode fiber filter[J]. *Acta Optica Sinica*, 2011, 31(8):0814006. (in Chinese)
- [26] ZHANG P, WANG T SH, MA W ZH, *et al.*. Tunable multiwavelength Tm-doped fiber laser based on the multimode interference effect[J]. *Applied Optics*, 2015, 54(15):4667-4671.
- [27] FU SH J, SHI G N, SHENG Q, *et al.*. Dual-wavelength fiber laser operating above 2  $\mu\text{m}$  based on cascaded single-mode-multimode-single-mode fiber structures[J]. *Optics Express*, 2016, 24(11):11282-11289.
- [28] WANG W, MENG H Y, WU X W, *et al.*. A nonlinear polarization rotation-based linear cavity waveband switchable multi-wavelength fiber laser[J]. *Laser Physics Letters*, 2013, 10(1):015104.

- [29] WANG X, ZHU Y D, ZHOU P, *et al.* . Tunable, multiwavelength Tm-doped fiber laser based on polarization rotation and four-wave-mixing effect[J]. *Optics Express*, 2013, 21(22) :25977-25984.
- [30] LIU P, WANG T SH, ZHANG P, *et al.* . Widely tunable multi-wavelength thulium-doped fiber laser based on nonlinear polarization rotation[J]. *Microwave and Optical Technology Letters*, 2016, 58(7) :1540-1543.
- [31] LIU X S, ZHAN L, LUO SH Y, *et al.* . Multiwavelength erbium-doped fiber laser based on a nonlinear amplifying loop mirror assisted by un-pumped EDF[J]. *Optics Express*, 2012, 20(7) :7088-7094.
- [32] LI Y, QUAN M R, TIAN J J, *et al.* . Tunable multiwavelength erbium-doped fiber laser based on nonlinear optical loop mirror and birefringence fiber filter[J]. *Applied Physics B*, 2015, 119(7) :363-370.
- [33] WANG P H, WANG L, SHI G H, *et al.* . Stable multi-wavelength fiber laser with single-mode fiber in a Sagnac loop[J]. *Applied Optics*, 2016, 55(12) :3339-3342.
- [34] DORAN N J, WOOD D. Nonlinear-optical loop mirror[J]. *Optics Letters*, 1988, 13(1) :56-58.

#### 作者简介:



石俊凯(1986—),男,天津宁河人,博士,助理研究员,2009年、2015年于天津大学分别获得学士、博士学位,主要从事光纤飞秒激光器及光梳测量方面的研究。E-mail:shijunkai@aoe.ac.cn



王国名(1986—),男,辽宁庄河人,硕士,助理研究员,2011年、2014年于长春理工大学分别获得学士、硕士学位,主要从事激光测量方面的研究。E-mail:wanguoming@aoe.ac.cn



纪荣祎(1983—),男,陕西渭南人,博士,副研究员,2006年于北京化工大学获得学士学位,2012年于北京理工大学获得博士学位,主要从事激光测量方面的研究。E-mail:jirongyi@aoe.ac.cn



周维虎(1962—),男,安徽无为,人,博士,研究员,博士生导师,1983年、2000年于合肥工业大学分别获得学士、博士学位,主要从事精密仪器与几何量计量方面的研究。E-mail:zhouweihu@aoe.ac.cn